

# A thermodynamic study on the interaction of nickel ion with myelin basic protein by isothermal titration calorimetry

G. Rezaei Behbehani · A. A. Saboury · L. Barzegar ·  
O. Zarean · J. Abedini · M. Payehghdr

Received: 7 July 2009 / Accepted: 3 November 2009 / Published online: 4 December 2009  
© Akadémiai Kiadó, Budapest, Hungary 2009

**Abstract** The interaction of myelin basic protein (MBP) from the bovine central nervous system with divalent nickel ion was studied by isothermal titration calorimetry at 37 and 47 °C in Tris buffer solution at pH = 7. The new solvation model was used to reproduce the heats of MBP + Ni<sup>2+</sup> interaction over the whole Ni<sup>2+</sup> concentrations. It was found that MBP has three identical and independent binding sites for Ni<sup>2+</sup> ions. The intrinsic dissociation equilibrium constant and the molar enthalpy of binding are 89.953 μM, −14.403 kJ mol<sup>−1</sup> and 106.978 μM, −14.026 kJ mol<sup>−1</sup> at 37 and 47 °C, respectively. The binding parameters recovered from the new solvation model were correlated to the structural changes of MBP due to its interaction with nickel ion interaction. It was found that in the low and high concentrations of the nickel ions, the MBP structure was destabilized.

**Keywords** Myelin basic protein · Nickel · Isothermal titration calorimetry · Binding parameters

## Introduction

Myelin is the multilamellar membranous sheath surrounding nerve axons and myelin basic protein (MBP) is an integral component of the myelin sheath in the central nervous system (CNS). It is the second most abundant protein in the CNS, comprising roughly 30% of the proteins found in CNS myelin. MBP is primarily located in the cytoplasmic spacing of the myelin sheath and is believed to play an active role in stabilizing the periodic myelin structure via non-specific interactions with the apposing lipid bilayers. MBP has been extensively studied as the autoantigen responsible for experimental autoimmune encephalomyelitis (EAE), a model for multiple sclerosis, that Multiple sclerosis (MS), for example, is an acquired CNS disorder of young adults and characterized by inflammatory demyelination as well as axonal degeneration [1–3]. The structure of the human MBP transcription until has been determined to consist of seven exons [4]. The 18.5 kDa isoform of MBP is one of the most abundant proteins of the myelin sheath of the adult mammalian CNS, and has been the most thoroughly studied because of its importance in maintenance of the stability of the sheath [5]. The functions both in membrane adhesion, and as a linker connecting the oligodendrocyte membrane to the underlying cytoskeleton. Based on various spectroscopic measurements, all known forms of MBP (both classic and Golli) belong to the class of intrinsically disordered proteins (IDPs), sometimes also called intrinsically unstructured protein [6]. The conformation of MBP is highly dependent on its environment, it is highly extended and flexible in aqueous solution. Aqueous solution of MBP from bovine brain alone exhibited a circular dichroism (CD) spectrum characteristic of random coil protein molecules without any apparent secondary structures.

---

G. Rezaei Behbehani (✉)  
Chemistry Department, Imam Khomeini International  
University, Qazvin, Iran  
e-mail: grb402003@yahoo.com

A. A. Saboury  
Institute of Biochemistry and Biophysics,  
University of Tehran, Tehran, Iran

G. Rezaei Behbehani · L. Barzegar · O. Zarean · J. Abedini ·  
M. Payehghdr  
Chemistry Department, Payam Noor University (PNU),  
Abhar, Iran

M. Payehghdr  
Chemistry Department, Payam Noor University (PNU),  
Karaj, Iran

However, attains ordered secondary structure in the presence of detergents and lipids. The detailed high-resolution tertiary structure of MBP is not known [7–9]. This protein is extremely cationic ( $PI \sim 10.6$ ), and exists as a number of charge isomers or components (named  $C_1$ – $C_8$ ) that are the result of myriad post-translational modifications, where  $C_1$  is the least modified and most highly positively charged [10, 11]. The energy of biochemical binding processes or molecular interactions at constant temperature are measured by Isothermal Titration Calorimetry (ITC) [12, 13]. ITC gives invaluable thermodynamics information about biomacromolecule–ligand interactions. During the last 2 years, we attempted to study the metal ion binding chemistry of different protein [14–19]. They will change the conformational stability and form aggregates. The importance of metal ions such as  $Ca^{2+}$ ,  $Mg^{2+}$ ,  $Cu^{2+}$ , and  $Co^{2+}$  in determining the stability of MBP by ITC is widely reported [20–25]. The interactions of Cd, Co, Cu, Hg, Mn, Pb, Zn, Ca, and Mg ions by isolated MBP of bovine central nervous system [CN] have been recently assessed by centrifugal equilibrium dialysis. Some metal ions ( $Zn^{2+}$ ,  $Co^{2+}$ , and  $Cu^{2+}$ ) inhibits dissociation of MBP from the membrane [26–28]. There are some approximations in previous theories which result in rough average values of binding parameters including a lot of errors. We have introduced new solvation model which enables us to determine the binding parameters with minimal errors. This model is able to correlate the binding parameters to the effect of metals on the stability of a protein in a very simple way that successfully applied to the analysis of  $Ni^{2+}$  binding MBP. As a clear understanding of operational stability constitutes an important goal in protein technology, our efforts aimed at elucidation of the structure stability using the new solvation theory.

## Materials and methods

Myelin basic protein (MBP; MW = 18.5 kDa) from bovine central systems (CNS) obtained from Sigma chemical Co. Nickel nitrate was purchased from Merk Co. All other materials and reagents were of analytical grade, and solutions were made in double-distilled water. Tris solutions with 30 mM concentration, pH = 7.0, was used as a buffer.

Isothermal Titration Calorimetry, ITC, measurements were carried out on a VP-ITC ultrasensitive microcalorimeter (MicroCal, Northampton, MA). The isothermal titration microcalorimetric experiments were performed with the four channel commercial microcalorimetric system, Thermal Activity Monitor 2277, Thermometric, Sweden. The titration vessel was made from stainless steel. Nickel nitrate solution (1 mM) was injected by use of a Hamilton syringe into the calorimetric titration vessel, which contained 1.8 mL MBP (27  $\mu$ M). Thin (0.15 mm

inner diameter) stainless steel hypodermic needles, permanently fixed to the syringe, reached directly into the calorimetric vessel. Injection of nickel nitrate solution into the perfusion vessel was repeated 30 times with 30  $\mu$ L per injection. The calorimetric signal was measured by a digital voltmeter that was part of a computerized recording system. The heat of each injection was calculated by the “Thermometric Digitam 3” software program. The heats of dilution of the metal ion solutions were measured as described above, except that MBP was excluded. The microcalorimeter was frequently calibrated electrically during the course of the study. The heats of MBP +  $Ni^{2+}$  interactions reported in Table 1. The molecular weight of MBP was taken to be 18.5 kDa.

**Table 1** Heats of  $Ni^{2+}$  + MBP interactions,  $q$ , at 310 K (▲) and 320 K (■)

$[Ni^{2+}] / \mu M$	$[MBP] / \mu M$	$q / \mu J (\blacktriangle)$	$q_{dilut} / \mu J (\blacktriangle)$	$q / \mu J (\blacksquare)$	$q_{dilut} / \mu J (\blacksquare)$
10.989	26.703	−1310	−33.0	−116.1	−24.6
21.739	26.413	−251.5	−63.3	−223.0	−47.3
32.258	26.129	−362.0	−91.1	−321.3	−68.1
42.553	25.851	−463.0	−116.7	−411.5	−87.2
52.631	25.579	−555.2	−140.0	−494.2	−104.8
62.500	25.312	−639.3	−161.3	−570.0	−120.9
72.165	25.051	−715.9	−179.9	−639.5	−135.7
81.633	24.796	−785.7	−196.8	−703.2	−149.3
90.909	24.545	−849.4	−212.4	−761.7	−161.8
100.000	24.300	−907.6	−226.6	−815.4	−173.3
108.911	24.059	−960.8	−239.6	−864.8	−183.9
117.647	23.823	−1009.5	−251.5	−910.4	−193.7
126.214	23.592	−1054.1	−262.4	−952.4	−202.7
134.615	23.365	−1095.1	−272.5	−991.3	−211.1
142.857	23.143	−1132.9	−281.8	−1027.3	−218.9
150.943	22.924	−1167.7	−290.4	−1060.7	−226.1
158.878	22.710	−1199.9	−298.3	−1091.7	−232.8
166.666	22.500	−1229.7	−305.7	−1120.6	−239.1
174.312	22.294	−1257.4	−312.6	−1147.5	−245.0
181.818	22.091	−1283.1	−319.0	−1172.7	−250.5
189.189	21.892	−1307.0	−324.9	−1196.2	−255.6
196.428	21.696	−1329.4	−330.6	−1218.3	−260.4
203.539	21.504	−1350.3	−335.8	−1239.0	−265.0
210.526	21.316	−1369.9	−340.7	−1258.5	−269.3
217.391	21.130	−1388.3	−345.3	−1276.8	−273.3
224.138	20.948	−1405.5	−349.7	−1294.1	−277.1
230.769	20.769	−1421.7	−353.8	−1310.4	−280.7
237.288	20.593	−1437.0	−357.7	−1325.8	−284.1
243.697	20.420	−1451.4	−361.4	−1340.4	−287.4
250.000	20.250	−1465.0	−364.8	−1354.2	−290.5

$q_{dilut}$  are the heats of dilution of  $Ni(NO_3)_2$  with water. The precision is  $\pm 0.1 \mu J$  or better

**Results and discussion**

We have shown previously [29–38] that the heats of the macromolecules + ligand interactions in the aqueous solvent systems can be calculated via the following equation:

$$q = q_{\max}x'_B - \delta_A^\circ(x'_A L_A + x'_B L_B) - (\delta_B^\circ - \delta_A^\circ)(x'_A L_A + x'_B L_B)x'_B \tag{1}$$

where  $q$  is the heat of MBP + Ni<sup>2+</sup> interaction at certain ligand concentrations and  $q_{\max}$  represents the heat value upon saturation of all MBP. The parameters  $\delta_A^\circ$  and  $\delta_B^\circ$  reflect to the net effect of Ni<sup>2+</sup> on the MBP stability in the low and high Ni<sup>2+</sup> concentrations, respectively.  $p > 1$  or  $p < 1$  indicate positive or negative cooperativity of macromolecule for binding with ligand, respectively;  $p = 1$  indicate that the binding is non-cooperative.  $x'_B$  can be expressed as follows:

$$x'_B = \frac{px_B}{x_A + px_B} \tag{2}$$

$x_B$  is the fraction of the Ni<sup>2+</sup> ions needed for saturation of the binding sites, and  $x_A = 1 - x_B$  is the fraction of unbounded Ni<sup>2+</sup> ions.  $x_B$  fractions can be expressed as follows:

$$x_B = \frac{[Ni^{2+}]_T}{[Ni^{2+}]_{\max}} \quad x_A = 1 - x_B \tag{3}$$

$[Ni^{2+}]_T$  total concentration of Ni<sup>2+</sup> and  $[Ni^{2+}]_{\max}$  is the maximum concentration of Ni<sup>2+</sup> ion upon saturation of all MBP. In general, there will be “ $g$ ” sites for binding of Ni<sup>2+</sup> per MBP molecule.  $L_A$  and  $L_B$  are the relative contributions due to the fractions of unbounded and bounded Ni<sup>2+</sup> in the heats of dilution in the absence of MBP and can be calculated from the heats of dilution of nickel nitrate solution in buffer,  $q_{\text{dilut}}$ , as follows:

$$L_A = q_{\text{dilut}} + x_B \left( \frac{\partial q_{\text{dilut}}}{\partial x_B} \right), \quad L_B = q_{\text{dilut}} - x_A \left( \frac{\partial q_{\text{dilut}}}{\partial x_B} \right) \tag{4}$$

The heats of MBP + Ni<sup>2+</sup> interactions,  $q$ , were fitted to Eq. 1 over the whole Ni<sup>2+</sup> compositions. In the fitting procedure the only adjustable parameter ( $p$ ) was changed until the best agreement between the experimental and calculated data was approached (Fig. 1). The small relative standard coefficient errors and the high  $r^2$  values (1) support the method. The binding parameters for MBP + Ni<sup>2+</sup> interactions recovered from Eq. 1 are listed in Table 2.

Consider a solution containing ligand, (Ni<sup>2+</sup>), and a macromolecule (MBP) that contains “ $g$ ” sites capable of binding the ligand. If the multiple binding sites on a macromolecule are identical and independent, the ligand binding sites can be reproduced by a model system of monovalent molecules (MBP<sub>g</sub> → gMBP) with the same set

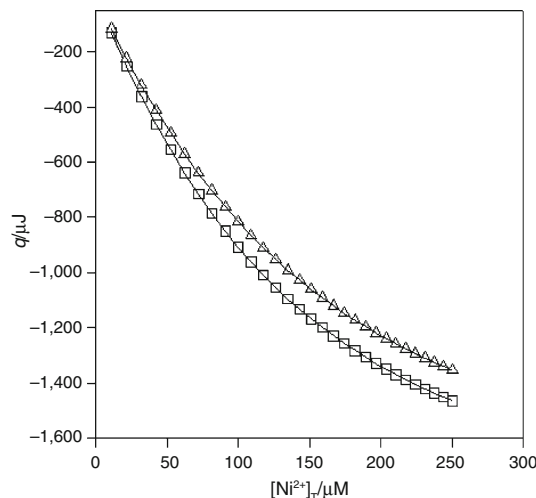


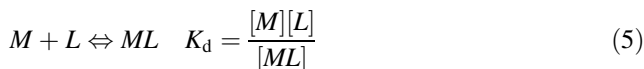
**Fig. 1** Comparison between the experimental heats for MBP + Ni<sup>2+</sup> interactions at 310 K (square), 320 K (triangle), and calculated data (lines) via Eq. 1. The  $[Ni^{2+}]_T$  are the total concentrations of Ni(NO<sub>3</sub>)<sub>2</sub> solutions in 1,000 μM

**Table 2** Binding parameters for MBP + Ni<sup>2+</sup> interactions via Eq. 1

Parameters	$T = 310$ K	$T = 320$ K
$K_d/\mu\text{M}$	89.953 ± 0.0038	106.978 ± 0.0053
$p$	1.20	1
$\delta_A^\theta$	-4.964 ± 0.037	-4.757 ± 0.010
$\delta_B^\theta$	-6.471 ± 0.030	-4.708 ± 0.013
$\Delta H_{\max} = \text{kJ mol}^{-1}$	-43.209	-42.078

$p$  Values (1 and 1 at 37 and 47 °C, respectively) suggest that Ni<sup>2+</sup> ions bind preferentially to the native state of MBP.  $\delta_A^\theta$  and  $\delta_B^\theta$  values for MBP + Ni<sup>2+</sup> interactions are negative at 37 and 47 °C (Table 2), indicating that in the low and maximum concentration of the nickel ions the MBP structure was destabilized as a result of binding to Ni<sup>2+</sup> ions

of dissociation equilibrium constant,  $K_d$ , values. Thus, the reaction under consideration can be written as:



For a set of identical and independent binding sites, we have shown before [12, 14, 16, 17, 39]:

$$\Delta H = \frac{1}{A_i} \left\{ (B + K_d) - \left[ (B + K_d)^2 - C \right]^{\frac{1}{2}} \right\} \tag{6}$$

$A_i$ ,  $B_i$ , and  $C_i$  are constants in each injection  $i$ , which have been defined as follows:

$$A_i = \frac{V_i}{2q_i} \quad B = g[M]_T + [L]_T \quad C = 4g[M]_T[L]_T \tag{7}$$

where  $V_i$  is the volume of the reaction solution in the calorimetric sample cell in each injection step.  $M_T$  is the total MBP concentration and  $L_T$  is the total Ni<sup>2+</sup>

concentration in the calorimetric sample cell in each injection step. Equation 6 contains two unknown parameters,  $K_d$  and  $\Delta H$ . A series of reasonable value for  $K_d$  is inserted into Eq. 6 and corresponding values for  $\Delta H$  are calculated and the graph  $\Delta H$  versus  $K_d$  is constructed. Curves of all titration steps will intersect in one point, which represents the precise value for  $\Delta H$  and  $K_d$ . The plots of  $\Delta H$  versus  $K_d$ , according to Eq. 6, for 30 injections are shown in Fig. 2.

It is possible to use Eq. 8 for calculation of  $K_d$ , and  $g$  in a very simple way as follows [13, 14]:

$$\frac{\Delta q}{q_{\max}} M_T = \left( \frac{\Delta q}{q} \right) L_T \frac{1}{g} - \frac{K_d}{g} \quad (8)$$

where  $\Delta q = q_{\max} - q$ . Therefore, the plot of  $(\Delta q/q_{\max})M_T$  versus  $(\Delta q/q)L_T$  should be a linear plot with a slope of  $(1/g)$  and a vertical intercept of  $(K_d/g)$ . The linear plot has been examined by different appraised values for  $q_{\max}$  to

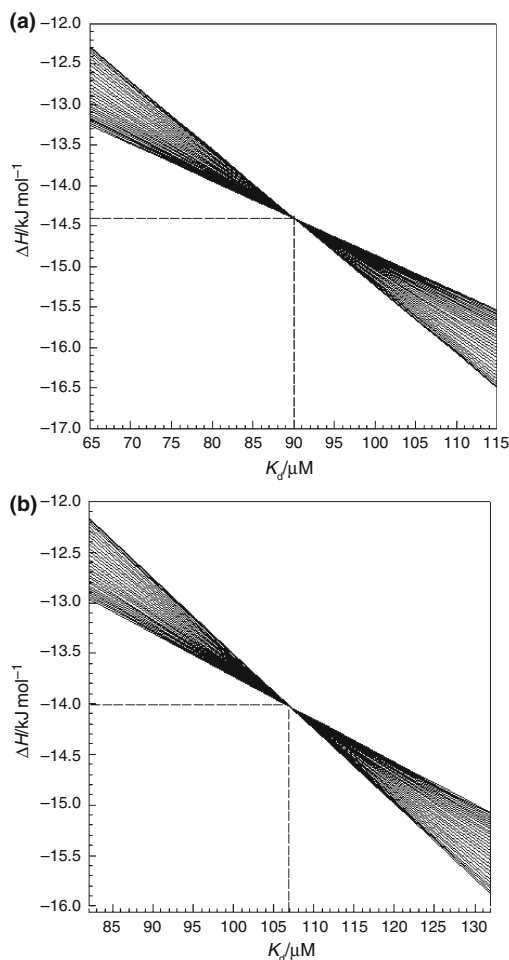


**Fig. 2** **a**  $\Delta H$  versus  $K_d$  for all 30 injections in the reasonable values of  $K_d$ , according to Eq. 6 at  $T = 310$  K. **b**  $\Delta H$  versus  $K_d$  for all 30 injections in the reasonable values of  $K_d$ , according to Eq. 6 at  $T = 320$  K

find the best value for the correlation coefficient (near to one). The best linear plots (Figs. 5 and 6) were obtained using a value of  $-2,100$  and  $-2,045 \mu\text{J}$  (equal to  $-43.209$  and  $-42.078 \text{ kJ/mol}$  at  $37$  and  $47$  °C, respectively) for  $q_{\max}$ . The amounts of  $g$  and  $K_d$ , obtained from the slope and vertical intercept plot, are  $3$  and  $89.953$  and  $106.978 \mu\text{M}$  at  $37$  and  $47$  °C, respectively. If  $q$  and  $q_{\max}$  are calculated per mole of biomacromolecule than the molar enthalpy of binding for each binding site ( $\Delta H$ ) will be  $\Delta H = q_{\max}/g$ . Dividing the  $q_{\max}$  value of  $-43.209$  and  $-42.078 \text{ kJ mol}^{-1}$  by  $g = 3$ , therefore, gives  $-14.403$  and  $-14.026 \text{ kJ mol}^{-1}$  at  $37$  and  $47$  °C, respectively.

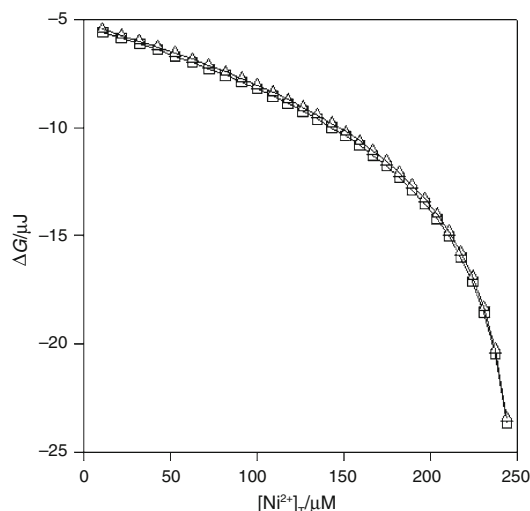


**Fig. 3** Comparison between the experimental Gibbs free energies at  $310$  K (square) and  $320$  K (triangle) for  $\text{Ni}^{2+}$  interactions and calculated data (lines) via Eq. 9

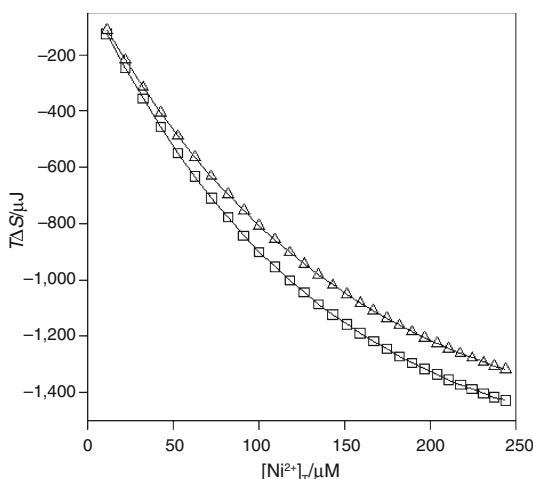


**Fig. 4** Comparison between the experimental entropies at  $310$  K (square) and  $320$  K (triangle) for MBP +  $\text{Ni}^{2+}$  interactions and calculated data (lines) via Eq. 9

The standard Gibbs free energies as a function of  $\text{Ni}^{2+}$  concentrations can be obtained as follows:

$$\Delta G^\circ = -RT \ln K_a \quad (9)$$

The standard Gibbs energies,  $\Delta G^\circ$ , calculated from Eq. 9 have shown graphically in Fig. 3.  $T\Delta S$  values were calculated using  $\Delta G^\circ$  values at different temperatures and have shown in Fig. 4.  $\delta_A^\theta$  and  $\delta_B^\theta$  values for MBP +  $\text{Ni}^{2+}$  interactions are negative at 37 and 47 °C (Table 2),

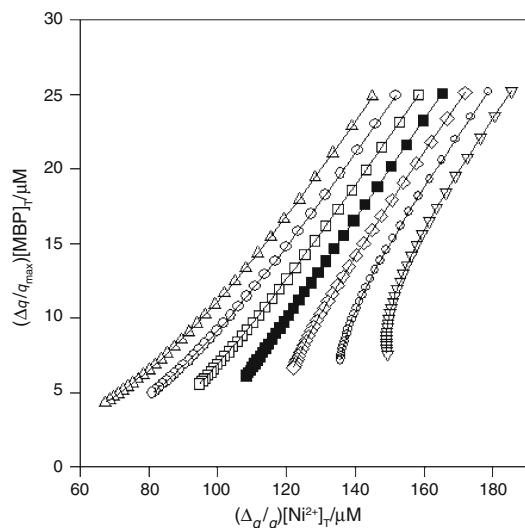


**Fig. 5** The best linear plot of  $(\Delta q/q_{\max})[\text{MBP}]_T$  versus  $(\Delta q/q)[\text{Ni}^{2+}]_T$  at 310 K, according to the Eq. 8, using a value of  $-2,100 \mu\text{J}$  for  $q_{\max}$  (■),  $-2,020 \mu\text{J}$  (□),  $-1,940 \mu\text{J}$  (○),  $-1,860 \mu\text{J}$  (△),  $-2,180 \mu\text{J}$  (◇),  $-2,260 \mu\text{J}$  (○),  $-2,340 \mu\text{J}$  (▽)

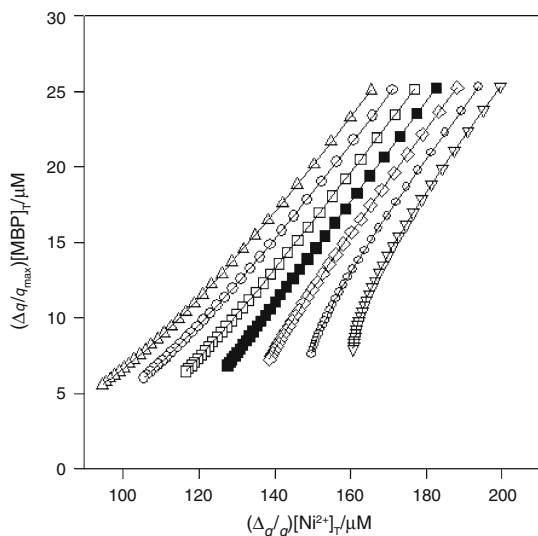


**Fig. 6** The best linear plot of  $(\Delta q/q_{\max})[\text{MBP}]_T$  versus  $(\Delta q/q)[\text{Ni}^{2+}]_T$  at 320 K, according to the Eq. 8, using a value of  $-2,045 \mu\text{J}$  for  $q_{\max}$  (■),  $-1,985 \mu\text{J}$  (□),  $-1,925 \mu\text{J}$  (○),  $-1,865 \mu\text{J}$  (△),  $-2,105 \mu\text{J}$  (◇),  $-2,165 \mu\text{J}$  (○),  $-2,225 \mu\text{J}$  (▽)

indicating that in the low and high concentration of the nickel ions, the MBP structure was destabilized as a result of binding to  $\text{Ni}^{2+}$  ions resulting in a decrease in its biological activity (Figs. 5, 6).

## Conclusions

The extended coordination model, via Eq. 1 reproduces satisfactorily the heats of MBP +  $\text{Ni}^{2+}$  interactions (Fig. 1). The binding parameters derived from the new solvation model were attributed to a structural change of MBP due to its interactions with nickel ion. The ability to predict of activity of protein, binding enthalpies and dissociated binding constant, make this theory the most powerful one. The results of this study are further evidence of a possible role of  $\text{Ni}^{2+}$  in adding to the stability of MBP and its function as an extrinsic protein of the myelin sheath in vitro. The MBP +  $\text{Ni}^{2+}$  interaction exhibit decrease the stability and biological activity of MBP in the low and high concentration of the nickel ion at 37 and 47 °C.

**Acknowledgements** Financial support from the Universities of Imam Khomeini International University, Tehran and payam noor (Abhar) are gratefully acknowledged.

## References

1. Polverini E, Fasano A, Zito F, Riccio P, Cavatorta P. Conformation of bovine myelin basic protein purified with bound lipids. *Eur Biophys J.* 1999;28:351–5.
2. Hu Y, Israelachvili J. Lateral reorganization of myelin lipid domains by myelin basic protein studied at the air–water interface. *Colloids Surf B Biointerfaces.* 2008;62:22–30.
3. Leder C, Schwab N, Ip CW, Kroner A, Nave KA, Dormair K, et al. Clonal expansions of pathogenic CD8+ effector cells in the CNS of myelin mutant mice. *Mol Cell Neurosci.* 2007;36:416–24.
4. Pribyl TM, Campagnoni CW, Kampf K, Kashima T, Handley VW, McMahon J, et al. The human myelin basic protein gene is included within a 179-kilobase transcription unit: expression in the immune and central nervous systems. *Proc Natl Acad Sci USA.* 1993;90:10695–9.
5. Libich DS, Hill CMD, Haines JD, Harauz G. Myelin basic protein has multiple calmodulin-binding sites. *Biochem Biophys Res Commun.* 2003;308:313–9.
6. Libich DS, Harauz G. Backbone dynamics of the 18.5 kDa isoform of myelin basic protein reveals transient  $\alpha$ -helices and a calmodulin-binding site. *Biophys J.* 2008;94:4847–66.
7. Rivas AA, Civera C, Ruiz-Cabello J, Castro RM. Interaction of bovine myelin basic protein with cholesterol. *J Colloid Interface Sci.* 1998;204:9–15.
8. Tzakos AG, Fuchs P, Van Nuland NAJ, Troganis A, Tselios T, Deraos S, et al. NMR and molecular dynamics studied of an autoimmune myelin basic protein peptide and its antagonist. *Eur J Biochem.* 2004;271:3399–413.
9. Libich DS, Harauz G. Solution NMR and CD spectroscopy of an intrinsically disordered, peripheral membrane protein: evaluation of aqueous and membrane-mimetic solvent conditions for

- studying the conformational adaptability of the 18.5 kDa isoforms of myelin basic protein (MBP). *Eur Biophys J*. 2008;37:1015–29.
10. Hill CMD, Haines JD, Antler CE, Bates IR, Libich DS, Harauz G. Terminal deletion mutants of myelin basic protein: new insights into self-association and phospholipids interactions. *Micron*. 2003;34:25–37.
  11. Hill CMD, Harauz G. Charge effects modulate actin assembly by classic myelin basic protein isoforms. *Biochem Biophys Res Commun*. 2005;329:362–9.
  12. Saboury AA. New methods for data analysis of isothermal titration calorimetry. *J Therm Anal Calorim*. 2003;72:93–103.
  13. Saboury AA. A review on the ligand binding studies by isothermal titration calorimetry. *J Iran Chem Soc*. 2006;3:1–21.
  14. Saboury AA, Atri MS, Sanati MH, Moosavi-Movahedi AA, Hakimelahi GH, Sadeghi M. A thermodynamic study on the interaction between magnesium ion and human growth hormone. *Biopolymers*. 2006;81:120–6.
  15. Saboury AA, Atri MS, Sanati MH, Sadeghi M. Application of a simple calorimetric data analysis on the binding study of calcium ions by human growth hormone. *J Therm Anal Calorim*. 2006;83:175–9.
  16. Saboury AA, Kordbacheh M, Sanati MH, Mizani F, Shamsipur M, Yakhchali MB, et al. Thermodynamics of binding copper ion by human growth hormone. *Asian J Chem*. 2005;17:2773–82.
  17. Saboury AA, Atri MS, Sanati MH, Moosavi-Movahedi AA, Haghbeen K. Effects of calcium binding on the structure and stability of human growth hormone. *Int J Biol Macromol*. 2005;36:305–9.
  18. Rezaei Behbehani G, Saboury AA. A new method for thermodynamic study on the binding of magnesium with human growth hormone. *J Therm Anal Calorim*. 2007;89:852–61.
  19. Rezaei Behbehani G, Saboury AA. Using a new solvation model for thermodynamic study on the interaction of nickel with human growth hormone. *Thermochim Acta*. 2007;452:76–9.
  20. Rezaei Behbehani G, Saboury AA, Fallah Bagheri A. A thermodynamic study on the binding of calcium ion with myelin basic protein. *J Solution Chem*. 2007;36:1311–20.
  21. Rezaei Behbehani G, Saboury AA, Fallah Bagheri A. A thermodynamic study on the binding of cobalt ion with myelin basic protein. *Bull Korean Chem Soc*. 2008;29:736–40.
  22. Rezaei Behbehani G, Saboury AA, Fallah Bagheri A, Abedini A. Application of an extended solvation theory to study on the binding of magnesium ion with myelin basic protein. *J Therm Anal Calorim*. 2008;93:479–83.
  23. Rezaei Behbehani G, Saboury AA, Fallah Bagheri A. A new approach for titration calorimetric data analysis on the binding of magnesium ion with myelin basic protein. *J Solution Chem*. 2008;37:1127–35.
  24. Rezaei Behbehani G, Saboury AA, Divsalar A. Thermodynamic study of the binding of calcium and magnesium ions with myelin basic protein using the extended solvation theory. *Acta Biochim Biophys Sin*. 2008;40:964–9.
  25. Saboury AA, Sarri-Sarraf N, Saidian S. Thermodynamics of binding copper ion by myelin basic protein. *Thermochim Acta*. 2002;381:147–51.
  26. Saboury AA. Application of a new method for data analysis of isothermal titration calorimetry in the interaction between human serum albumin and  $\text{Ni}^{2+}$ . *J Chem Thermodyn*. 2003;35:1975–81.
  27. Earl C, Chantry A, Mohammad N, Glynn P. Zinc ions stabilize the association of basic protein with brain myelin membranes. *J Neurochem*. 1988;51:718–24.
  28. Berlet HH, Bischoff H, Weinhardt F. Divalent metals of myelin and their differential binding by myelin basic protein of bovine central nervous system. *Neurosci Lett*. 1994;179:75–8.
  29. Rezaei Behbehani G. A high performance method for thermodynamic study on the binding of copper ion and glycine with Alzheimer's amyloid  $\beta$  peptide. *J Therm Anal Calorim*. 2009;96:631–5.
  30. Rezaei Behbehani G, Divsalar A, Saboury AA, Hekmat A. A thermodynamic study on the binding of PEG-stearic acid copolymer with lysozyme. *J Solution Chem*. 2009;38:219–29.
  31. Rezaei Behbehani G. A novel method for thermodynamic study on the binding of copper ion with Alzheimer's amyloid  $\beta$  peptide. *Chin Sci Bull*. 2009;54:1037–42.
  32. Rezaei Behbehani G, Saboury AA, Ganjali MR, Faridbod F. A high performance theory for thermodynamic study on the binding of human serum albumin with erbium chloride. *Chin J Chem*. 2009;27:289–94.
  33. Rezaei Behbehani G, Saboury AA, Divsalar A. Using the extended solvation theory for thermodynamic study on the interaction of magnesium and cobalt ions with human growth hormone. *J Korean Chem Soc*. 2008;52:1–6.
  34. Rezaei-Behbehani G. A predictive, simple and rapid method for thermodynamic study on the binding of copper ion with Alzheimer's amyloid  $\beta$  peptide. *Chin Chem Lett*. 2009;20:751–4.
  35. Rezaei Behbehani G, Divsalar A, Saboury AA. A high performance method for thermodynamic study on the binding of human serum albumin with erbium chloride. *J Therm Anal Calorim*. 2009;96:663–8.
  36. Rezaei Behbehani G, Saboury AA, Taleshi E. A comparative study on direct calorimetric determination of denaturation enthalpy for lysozyme in sodium dodecyl sulfate and dodecyltrimethylammonium bromide. *J Solution Chem*. 2008;37:619–29.
  37. Rezaei Behbehani G, Saboury AA, Taleshi E. Determination of partial unfolding enthalpy for lysozyme upon interaction with dodecyltrimethylammoniumbromide using an extended solvation model. *J Mol Recognit*. 2008;21:132–5.
  38. Rezaei Behbehani G, Waghome EW. A high-performance theory for thermodynamic study of solvation in mixed solvents. *Thermochim Acta*. 2008;478:1–5.
  39. Saboury AA. A simple method for determination of binding isotherm by isothermal titration calorimetry and its application to the interaction between  $\text{Cu}^{2+}$  and myelin basic protein. *J Therm Anal Calorim*. 2004;77:997–1004.